Workflow for monitoring gravitational focal length changes of the HartRAO 26 m radio telescope's main reflector

Theresa PFAFFINGER, Axel NOTHNAGEL and Christoph HOLST, Germany

Key words: Laser Scanning, Radio Telescopes, Deformation Analysis, VLBI

SUMMARY

Several telescope-related effects can interfere with VLBI (Very Long Baseline Interferometry) measurements and influence the signal path of the received radio signal. This, in turn, has an impact on the calculation of the station coordinates of the VLBI telescope and additional results that are calculated using VLBI observations, such as Earth rotation parameters or the International Terrestrial Reference Frame (ITRF). It is therefore necessary to determine such effects and correct the signal path for each individual VLBI observation. In addition to temperature influences, gravitational effects have a significant impact on the delay of the incoming signal. One gravitational effect is the overall deformation of the main reflector. For most telescopes, the main reflector has the shape of a rotational paraboloid with only the focal length describing its appearance. Consequently, changes in the focal length affect the length of the signal path and must therefore be determined to correct the delay observations.

This study investigates gravitational focal length changes of the 26 m radio telescope at the Hartebeesthoek site (HartRAO) in South Africa. It belongs to the South African Radio Astronomy Observatory (SARAO). For this purpose laser scan data of 88 different telescope positions as two-face measurements were recorded in April 2024. In contrast to other deformation monitoring tasks, the null hypothesis is that the shape of the object is a rotational paraboloid when pointing at zenith, while in other positions this shape is kept as much as the construction constraints permit.

Some results under the question of deformation analysis of the HartRAO radio telescope have already been discussed in Pfaffinger et al. (2025). Differing from this past publication, our present study deals with the measurement concept and the analysis with special focus on the characteristics of the HartRAO 26 m radio telescope, unstable scanning results and focal length variations dependent on the elevation angle. The analysis reveals local surface deformations, including noticeably tilted panels, and shows that the focal length increases with elevation. The method's repeatability equals 0.6 mm, as measured from the standard deviation of several zenith positions.

Workflow for monitoring gravitational focal length changes of the HartRAO 26 m radio telescope's main reflector

Theresa PFAFFINGER, Axel NOTHNAGEL and Christoph HOLST, Germany

1. INTRODUCTION

In Very Long Baseline Interferometry (VLBI), radio telescopes receive signals from extragalactic radio sources in space, which are almost infinitely far away. A pair of radio telescopes on the Earth´s surface simultaneously receives the signal from the same radio source. Through exact time measurements via atomic clocks and some physical relations between time, distance, and velocity, the distance between the reference points of the two radio telescopes can be calculated with a high accuracy level in the range of some millimeters in the best case (Nothnagel, 2020).
High stability of the receiving unit is required when receiving the signal to reach this level of accuracy. Various influencing factors on the radio telescope can disturb the stability and thus cause signal path variations. For example, thermal effects can lead to surface expansions that deflect the signal. These effects have already been analyzed in the past for several telescopes (Nothnagel, 2009).
Next to the thermal influences, gravitational effects cause signal path variations. The telescope's main reflector, which is often constructed as a paraboloid of revolution, is "considered in a stable gravitational state when it points to zenith (90° elevation angle) because the forces act radially symmetrically around the optical axis" (Nothnagel et al., 2019). When the inclination of the telescope towards the horizon changes, the structure deforms due to gravity and, to first order, changes the focal length of the paraboloid. The signal path is affected in particular by these variations, as well as by displacements of the vertex, which is the symmetry center of the main reflector, and changes in the distance between the vertex and the sub reflector in the different observation positions of the radio telescope (Clark & Thomsen, 1988). The resulting signal path variations mainly affect the height component of the telescope reference point, which in turn influences the scale factor of the VLBI frame. In the example of the telescopes in Medicina and Noto, the height change is in the mm range (Sarti et al., 2010).
In this study, we are dealing with focal length variations and local surface deformations of the main reflector of the HartRAO 26 m radio telescope in different telescope positions. We will derive the following research contributions within this study:

1. Introducing a workflow that uses laser scans to determine focal length variations and local surface deformations
2. Developing a strategy for dealing with systematic effects that are caused by laser scanner misalignments
3. Analyzing the relation between focal length variation and elevation angle of the radio telescope

The measurement setup and initial results have already been presented in Pfaffinger et al. (2025). The novelty of this paper lies in providing deeper insight into the radio telescope itself, discussing unstable scans in more detail, and presenting focal lengths as a function of elevation as new results.
Therefore in the following, first, we introduce some previous studies investigating deformations of other radio telescopes (Chapter 2). Chapter 3 gives a deeper introduction to the HartRAO 26 m telescope, especially its construction. Chapter 4 describes the measurement concept for laser scanner measurements. Herein, we also analyze systematic effects due to the unstable mounting of the laser scanner. We analyze the results in Chapter 5. A conclusion will follow in Chapter 6.

2. STATE-OF-THE-ART

In 1988 Clark and Thomsen (1988) did the first deformation analysis for VLBI antennas using the example of the 85 ft. antenna in Fairbanks, Alaska. They mention deformations caused by gravity loads, temperature, and wind, and introduce the parametrization of the main reflector as a paraboloid of revolution with

$$\frac{X_j^2 + Y_j^2}{4f} = Z_j \,, \tag{1}$$

where $(X_j, Y_j, Z_j)^T$ are the Cartesian coordinates (with $j = 1, \dots, m$ number of points) with the origin in the vertex of the paraboloid of revolution $(0,0,0)^T$, and f is the focal length.
Sarti et al. (2009) and Holst et al. (2012) follow the observations from Clark and Thomsen (1988) and use the paraboloid parameterization for further studies in deformation analysis of radio telescopes. Both are using laser scan data to get focal length changes of the 32 m antennas in Medicina and Noto in Italy (Sarti et al., 2009) and the 100 m antenna in Effelsberg in Germany (Holst et al., 2012). Whereas Holst et al. (2012) fixed the scanner upside down at the sub reflector to cover the whole main reflector in one scan, Sarti et al. (2009) put the scanner close to the vertex of the main reflector and scanned from two different positions to get one scan for the whole paraboloid.
In order to transform the point clouds into the coordinate system given in Equation (1), we further introduce three translation parameters $\Delta\boldsymbol{X} = (\Delta X, \Delta Y, \Delta Z)^T$, to transform the scanner reference point to the vertex of the main reflector, and two rotation parameters Φ_x and Φ_y, to fulfill the transformation from the scanner system $\boldsymbol{x_j}$ to the telescope system $\boldsymbol{X_j}$ (Holst et al., 2012; Holst et al., 2019), with

$$\boldsymbol{X_j} = \left(X_j, Y_j, Z_j\right)^T = \boldsymbol{R}_y\left(\Phi_y\right)\boldsymbol{R}_x(\Phi_x) \cdot \boldsymbol{x_j} + \Delta\boldsymbol{X} \,. \tag{2}$$

Laser scanners suffer from misalignments leading to wrong results for focal length estimations. Holst et al. (2019) found out that either combining two-face measurements or an in situ calibra-

tion of the data will reduce the effects of the scanner misalignments. Thus, this step is essential for an unbiased deformation analysis of the main reflector.
Also, for some photogrammetric approaches for determining focal length changes, parameterization as a paraboloid builds the basis for the analysis, e.g., for Fraser (1986).
Recently, Lösler et al. (2025) dealt with signal path variations of the 26 m radio telescope at the Mount Pleasant Radio Observatory Hobart (Tasmania, Australia). For their approach, they used a combination of cameras and UAVs for collecting data and Zernike polynomials for modelling the results.

3. INVESTIGATED TELESCOPE: HartRAO 26 m radio telescope at Hartebeesthoek Site

For this study, we investigate the HartRAO 26 m radio telescope that is located at the Hartebeesthoek site, north-west of Johannesburg in South Africa (National Research Foundation, 2026b). Hartebeesthoek site belongs to the South African Radio Astronomy Observatory (SARAO), a facility of the National Research Foundation. The 26 m radio telescope and another 15 m radio telescope for astronomy and geodesy, a Satellite Laser Ranger (SLR) for geodesy, and GNSS-receivers for GPS, GLONASS, and Galileo are arranged there (National Research Foundation, 2025a).
Together with 37 other currently observing VLBI antennas of the IVS (International VLBI Service), it serves telescope coordinates, Earth Rotation Parameters, and the position of radio sources (International VLBI Service for Geodesy and Astrometry, 2026; Nothnagel, 2020). Most observing antennas have an azimuth-elevation (alt-azimuth) mount, whereas the HartRAO telescope has an equatorial mount. (Cheng, 2009; International VLBI Service for Geodesy and Astrometry, 2026; Nothnagel, 2009).

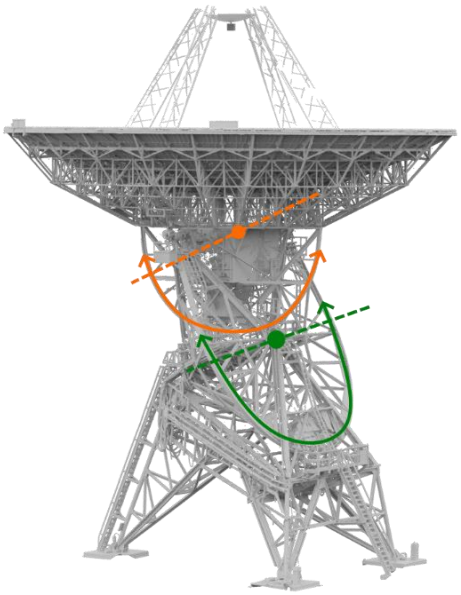

Figure 1: 3D-model of the 26 m HartRAO radio telescope - green: HA-axis, orange: DEC-axis (adapted from Pfaffinger et al. (2025))

The HartRAO 26 m telescope can move around two axes, the hour-angle-axis (HA) and the declination-axis (DEC). The HA-axis is the primary axis of the radio telescope and is defined as parallel to the Earth's rotation axis. The DEC-axis is the secondary axis and perpendicular to the HA-axis, as Figure 1 depicts. The telescope is limited in moving into different observing positions to an HA from -88° to 88° and DEC from -88° to 45° (International VLBI Service for Geodesy and Astrometry, 2026).
The telescope is designed as a Cassegrain telescope. This means the main reflector has the shape of a paraboloid of revolution, and the sub reflector has the shape of a hyperboloid (Nothnagel, 2020). The diameter D of the main reflector, that is defined as 85 ft or 25.9 m, and the focal ratio (f/D) of 0.424 leads to a nominal focal length f of 10.9816 m in zenith position (National Research Foundation, 2025b). The shape of a paraboloid of revolution can be parameterized by the focal length f as described in Equation (1).
The main reflector can be divided into 252 panels of solid aluminum. They are arranged in seven concentric rings. Figure 2 shows a sketch of the main reflector, including the arrangement of the panels on the left. As one can see, not all of them are the same size. The right side of Figure 2 contains a photo of the main reflector in zenith position, where one can also see the feed horn system in the center of the main dish, the sub reflector above which can easily be recognized with some photogrammetric targets for past measurements on it, and the quadruped legs that are holding the sub reflector.
This radio telescope had its first operational day on 1 July 1961. In 2008, the telescope had to stop its VLBI observations because of a broken bearing. It took 21 months till the telescope could start driving again in July 2010 (Combrinck et al., 2011).
As the telescope is of considerable age and has already suffered a bearing failure, an investigation of its stability is necessary. In contrast to most of the telescopes introduced in Chapter 2, this instrument operates as a function of hour angle (HA) and declination (DEC) rather than

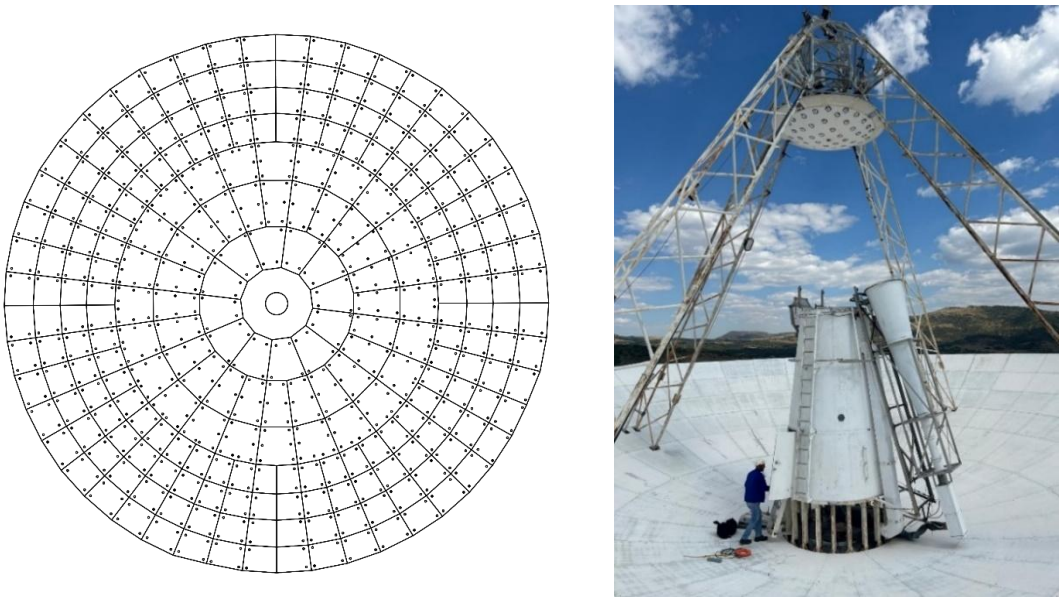

solely along elevation. As a result, a new concept must be developed to adequately account for

Figure 2: Sketch of the main reflector (created by Lia Lopez Mendoza) (left), photo of the main reflector including the feedhorn system and the sub reflector (right)

the telescope's different pointing positions. Therefore, we adapt the already known workflow from Holst et al. (2019) to get focal length changes of the telescope, representing the main reflector's shape.

4. WORKFLOW FOR DETECTING DEFORMATIONS OF THE MAIN REFLECTOR

We captured the surface with a laser scanner to analyze the deformations of the main reflector of the 26 m HartRAO radio telescope. This data is used to estimate local surface deformations and changes in focal length for different telescope positions. Therefore, we first introduce the measurement concept (Section 4.1). Afterwards, the data analysis presents the workflow to estimate the deformations of the main reflector (Section 4.2).

4.1 Measurement Concept

To ensure complete and reliable data collection, which forms the basis for all subsequent calculations, the individual steps must be carefully planned. Therefore, we firstly introduce the measurement schedule, followed by the setup of the laser scanner and the selected scan settings. Although Pfaffinger et al. (2025) have already described these aspects in detail, we briefly summarize them here to ensure clarity and coherence in the subsequent analyses. Finally, we will have a closer look at scans that show systematic errors caused by an unstable scanner mounting, which are excluded from further analysis.

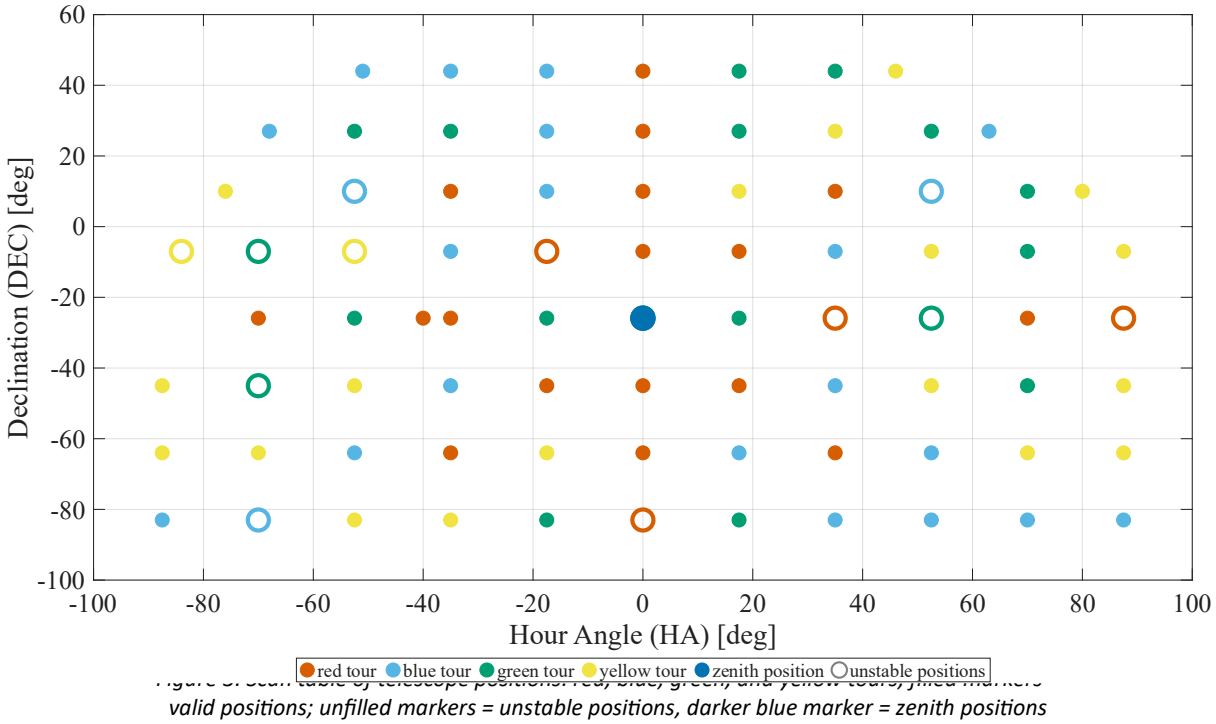

valid positions; unfilled markers = unstable positions, darker blue marker = zenith positions

4.1.1 Measurement schedule

To get an overall deformation model for the telescope, it is necessary to cover the full field-of-view of the HartRAO radio telescope. Therefore, we designed the schedule depicted in Figure 3, which contains a grid of positions within the HA and DEC limits of the radio telescope, shown.
The colors red, blue, green, and yellow indicate the respective tours scanned on four consecutive days from the 19th to the 22nd of April 2024. Due to incoming sunlight during the day and forming dew at night, the scanning time was limited from 6 p.m. to 11 p.m. Thus, the separation into four tours was necessary.
Valid scanning positions are shown as filled markers in the four different colors. The unfilled markers were found to be unstable scans during the evaluation, which is why they were excluded from the evaluation. This will be discussed in more detail in Section 4.1.3.
The darker blue dot in the center shows the zenith position of the telescope with an HA of 0° and a DEC of -25.89°. This position is scanned twice in each tour as a control measure in the adjustment.
For more details concerning the measurement concept, have a look at Pfaffinger et al. (2025).

4.1.2 Laser scanner mounting and settings

For the scanning process, we used the laser scanner *Imager 5016a* from the manufacturer *Zoller&Fröhlich*. It is mounted upside down at the sub reflector, at a special hinge system shown in Figure 4.
The hinge system acts like a two-axis gimbal that allows the scanner to point to nadir all the time due to its weight. An additional integrated brake ensures the mounting cannot move during scanning. The mounting is explained in more detail in Pfaffinger et al. (2025).
The mounting was modeled after the design of Holst et al. (2012) and allows the entire main reflector to be captured in a single scan. Unlike the approach of Sarti et al. (2009), there is no longer any need for control points to combine scans from multiple positions, as all relevant data is already contained in a single scan. The only data loss in the scans is shadowing caused by the feed horn and the quadruped legs. However, this is negligible.
For the scanning process, we chose a resolution of 6.3 mm at a distance of 10 m and normal quality, which takes around 3 minutes per scan.
Each position of the telescope shown in the scan table in Figure 3 is scanned twice, including two faces. The first scan is called cycle 1 and is defined from a horizontal angle of 0° to 180° and a full vertical angle of 0° to 360°. Cycle 2 is then defined as a horizontal angle from 180° to 360° and a full vertical angle from 0° to 360°. The two cycles contain the whole point cloud in face 1 and face 2, where both cycles consist of both face 1 and face 2. The amount of face 1 and face 2 parts depends on the telescope's position. Measuring in face 1 and face 2 is necessary

as one way to deal with the systematic effects of the laser scanner misalignments, as Holst et al. (2019) showed.

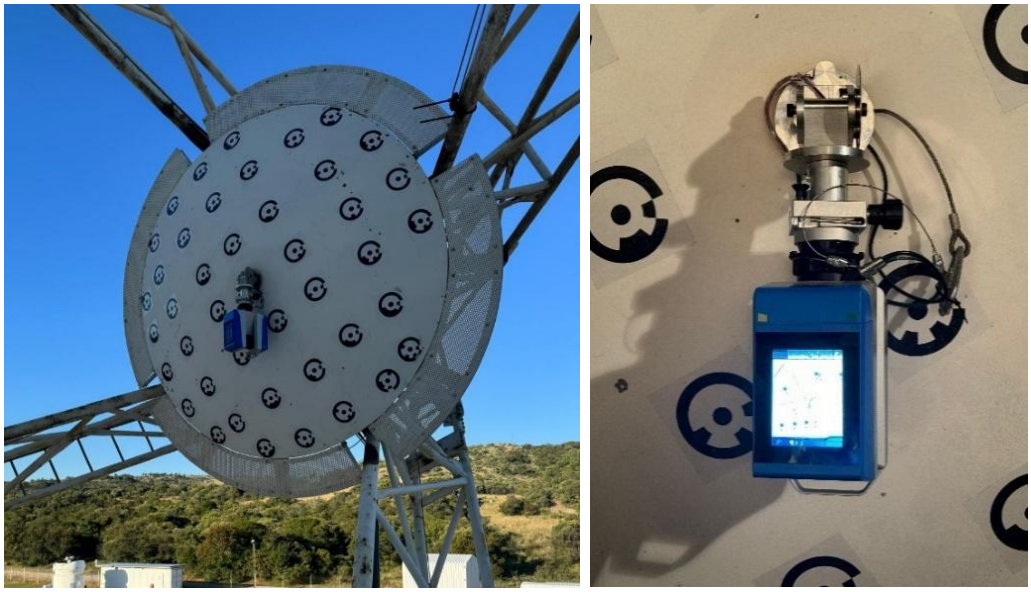

Figure 4: Scanner mounted at the sub reflector (left), scanner and hinge system (right) with the telescope in the scanner mounting position (HA: -89°, DEC: -1.5°)

4.1.3 Unstable scans

During the data evaluation, we identified a large amount of systematic effects in some of the laser scans. Those effects, as Figure 5 depicts, cannot be assigned to the aforementioned well-known laser scanner misalignments. Instead, the systematics are of larger magnitude (around

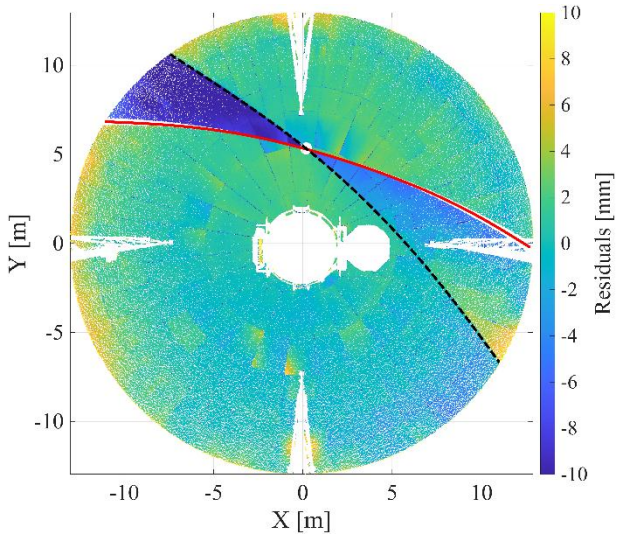

Figure 5: Residuals of unstable scan r5 cycle 1 (HA: 35°, DEC: -25.89°)

1 cm) and offer a different spatial pattern. Based on thorough analysis, we assume that they originate from unexpected movements of the sub reflector or a combined movement of the main and sub reflector, all while scanning.
In the analysis, this is clearly visible in the residuals shown in Figure 5. For example, for the unstable scan in position r5 for cycle 1, one can see along the black dotted line the shift in the data. The red line shows the border between the horizontal angles 0° and 180°, where the systematic effects of the laser scanner would appear. However, since the other effects are much larger, these come to the foreground here.
As these influences are way larger than the expected deformation, they affect the analysis significantly, and therefore, we eliminate the unstable scans from all further calculations (see Figure 3). As written before, we always require scans in two faces in order to minimize systematic effects caused by laser scanner misalignments. Consequently, if one cycle is affected, the corresponding second face is missing, which makes the second cycle unusable when applying the two-face method. Therefore, both cycles in a position are excluded if one of the two cycles is unstable. As a result, 12 out of the 88 positions cannot be further utilized, reducing the dataset to 76 positions.

4.2 Data analysis

Figure 6 shows the workflow that describes the entire process, where we combine cycle 1 and cycle 2 as two-face measurements to eliminate the systematic effects of the laser scanner misalignments. Contrary to Pfaffinger et al. (2025) in this study, we are not focusing on the calibration method anymore because the two-face method is more convenient and delivers the same results as Holst et al. (2019) show.
In detail, the first step of the workflow shown in Figure 6 is scanning one position in two cycles as described in Section 4.1. The captured point clouds are then cleaned in a three-step algorithm, including thresholding and plane estimation with RANSAC.
Afterwards, we use the scans to fit a rotational paraboloid as parameterized in Equations 1 and 2. The paraboloid fitting is done for each cycle separately. The results are residuals and a focal length for each cycle, each position. The two cycles are combined for each position by aligning their orientation and by building the mean values of the residuals and the focal lengths.
For each position, there are finally residuals that describe the local surface deformations of the main reflector, and a focal length that describes the overall shape of the main reflector. As this is done for all 76 positions, we can compare the focal length changes depending on the elevation afterwards.

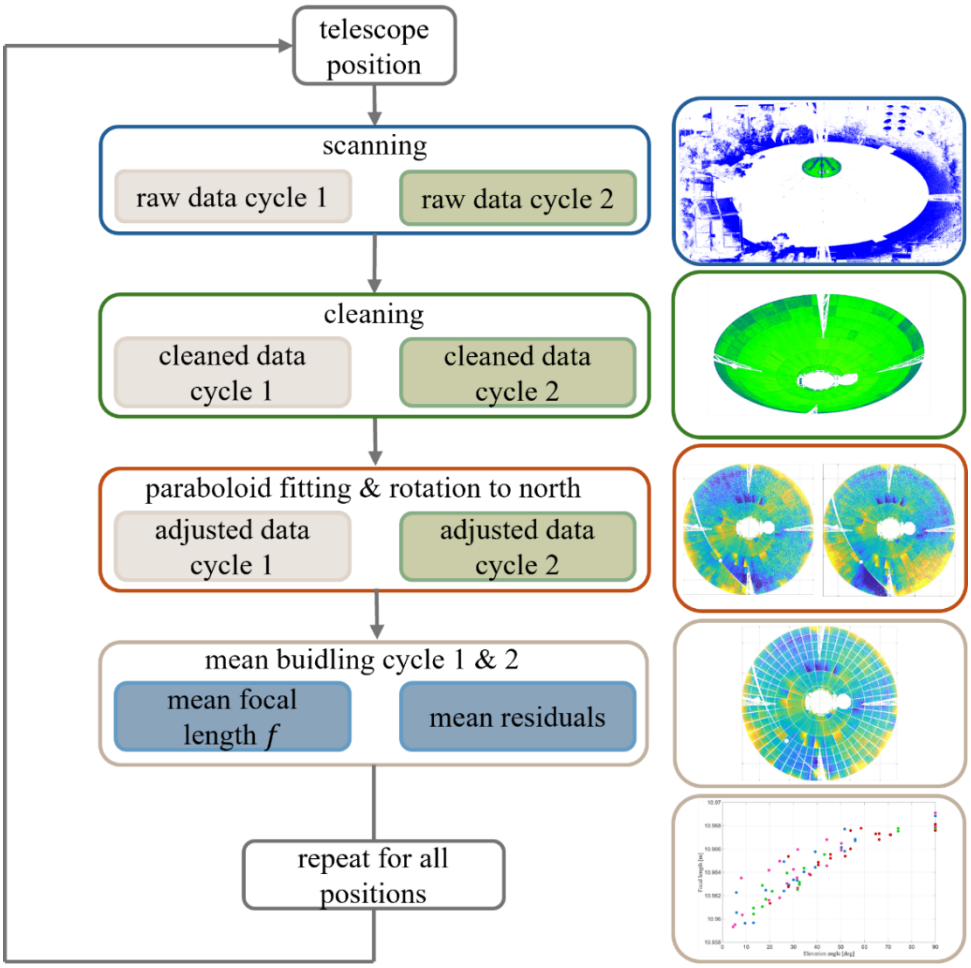

Figure 6: Workflow for quantifying deformations of the main reflector using laser scan data

5. RESULTS

This section shows the results using the combination of two face measurements to eliminate the effects of laser scanner misalignments. Special focus is put on the residuals, as they clearly show a reduction of systematic effects on the scanning data (Section 5.1). Furthermore, the focal length changes of the scanned positions are analyzed depending on the elevation of the position (Section 5.2).

5.1 Local surface deformations

To get some insight into the local surface deformations of the main reflector of the HartRAO 26 m radio telescope, the residuals of the least squares adjustment are used. They directly show the difference between a perfectly shaped paraboloid and the scanned telescope data that represents reality. Figure 7 shows the residuals of the adjusted data of position r23 as an

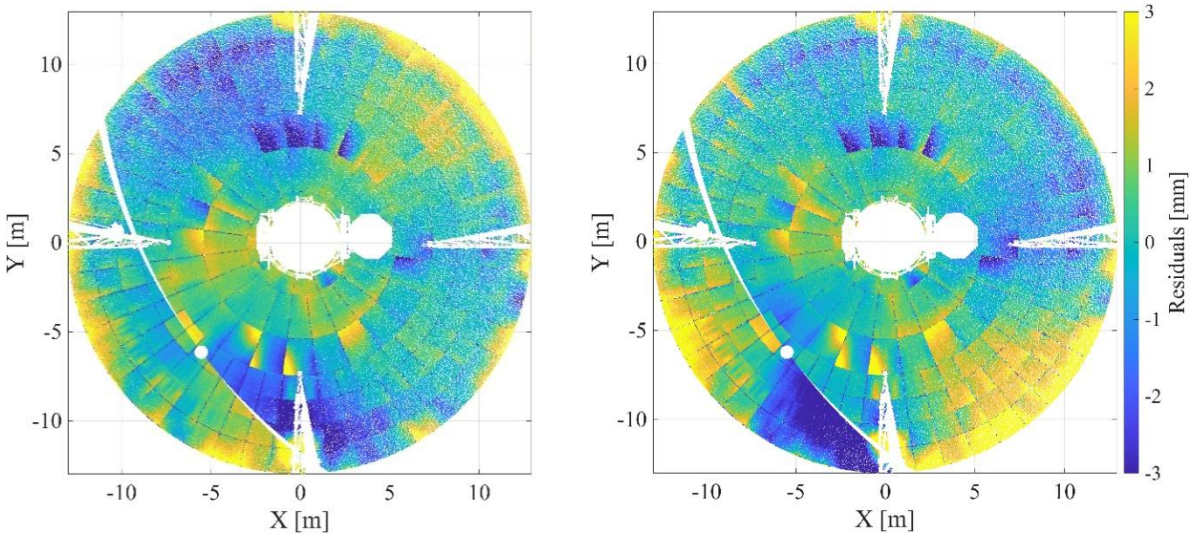

Figure 7: Residuals of scan r23 (HA: -35°, DEC: -64°), cycle 1 (left), cycle 2 (right) (adapted from Pfaffinger et al. (2025))

example for cycle 1 and cycle 2 separately. The systematic effects are clearly visible along the data gap that represents the horizontal angle equal to zero. The effects are flipped for cycle 1 and cycle 2, as the two-face sensitive effects flip their sign for face 1 and face 2.

To minimize the systematic effects of the laser scanner misalignments, we build the mean of cycle 1 and cycle 2 according to Figure 6. For the averaging, we calculate the mean individually for each panel in circles with a diameter of 10 cm. This leads to the final result for the residuals for position r23 in Figure 8. Here, the systematic effects are minimized significantly. Building the mean of the two faces is a reliable way to minimize the systematic effects of the laser scanner. As one can see clearly, there are some panels that are tilted, and some are also completely below the perfect paraboloid model. For the tilted panels, this is a clear hint that some screws are not fixed correctly. It is important to note that the axis limits of the residuals have been reduced from ±10 mm to ±3 mm compared to Figure 5.

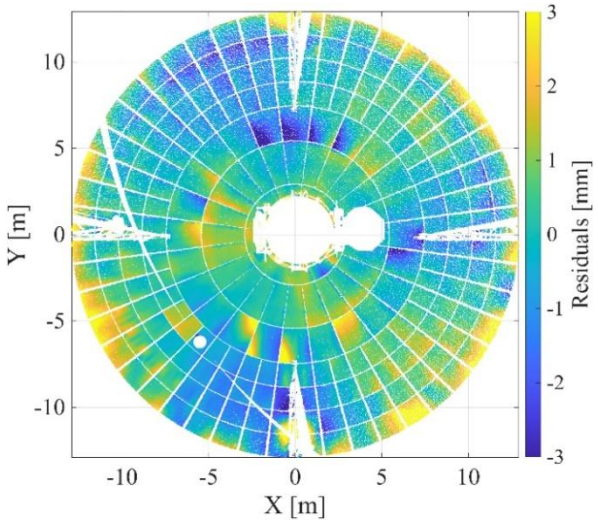

Figure 8: Mean residuals for position r23 (HA: -35°, DEC: -64°)

5.2 Elevation-dependent focal length variations

Besides the local surface deformations represented by the residuals, the focus lies on the focal length changes of the different telescope positions that describe the overall shape of the main reflector. The focal length changes affect the signal path and therefore have a great impact on VLBI calculations. As one parameter of the least squares adjustment for each cycle in each position, a focal length is calculated. Also, here we combine the focal length of cycle 1 and cycle 2 by building the mean value to minimize systematic effects of the laser scanner misalignments, as it is done for the residuals.
Figure 9 shows the estimated focal lengths for the 76 scanned positions of the telescope, dependent on the elevation. We calculate the elevation from the HA and the DEC. It can be seen that there is a trend that the focal length increases with a higher elevation angle with a maximum amount of around 10 mm. Herein, focal length estimations spread around this trend with about 2 mm. Looking at the multiple scanned zenith positions with an elevation angle of 90°, one can see that the focal lengths vary by 1.5 mm peak to peak. The standard deviation of the seven zenith positions of 0.6 mm represents the repeatability of the method used.
As expected, the focal lengths show a trend with increasing elevation, but not a strict pattern. This behaviour is consistent with the telescope's structural design, and future investigations will therefore examine the focal length variations also as a function of hour angle (HA) and declination (DEC).

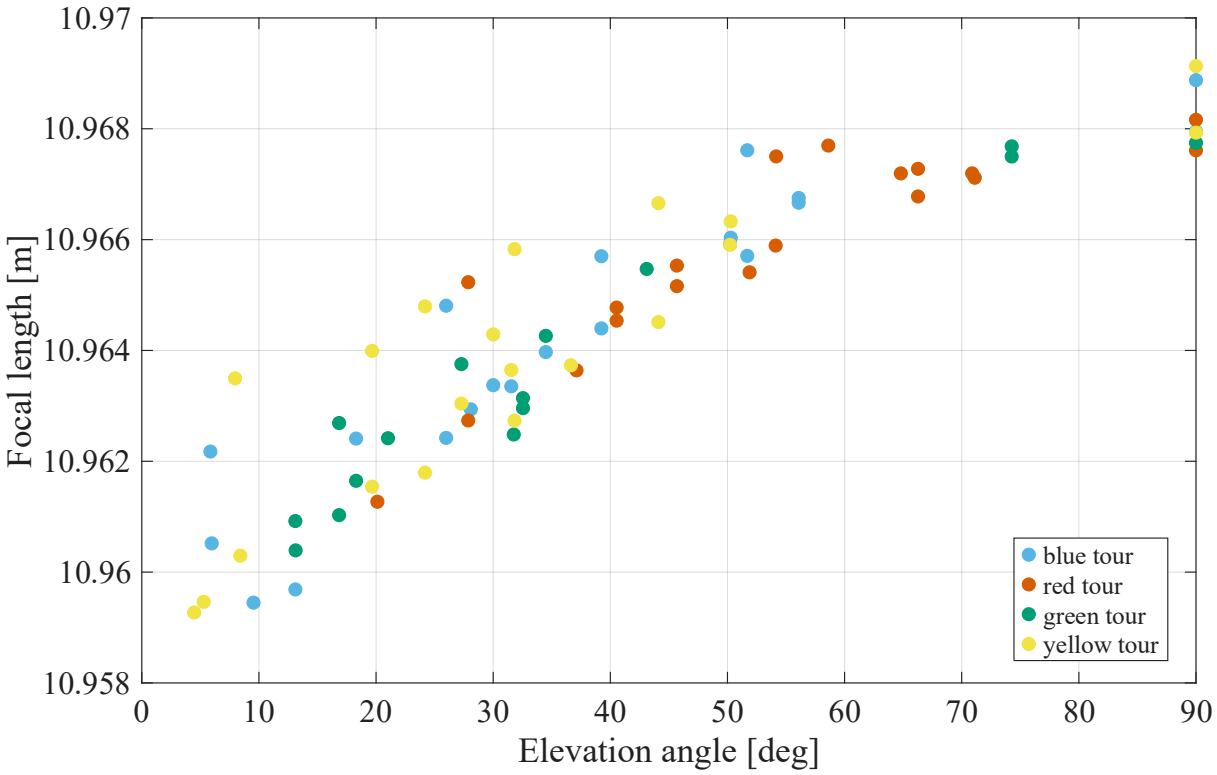

Figure 9: Elevation-dependent focal lengths

6. CONCLUSION

In this paper, we introduce a workflow both for estimating local surface deformations and focal length changes of the main reflector of the HartRAO 26 m radio telescope. Using two-face measurements, the systematic effects of the laser scanner misalignments are minimized. Attention is required during the evaluation process, as some scans are unstable and cannot be used for further evaluation because they distort the overall results. Therefore, manual sorting based on the results is necessary.
It is shown that focal lengths increase with a higher elevation and have a repeatability of 0.6 mm, represented by the standard deviation of the zenith positions.
In the next steps, the relationship between the changes in focal length and the position of the telescope will be examined in more detail in order to establish a connection to hour angle and declination. In addition, the local surface deformations will be examined in more detail, panel by panel.

FUNDING

This research was partly funded by German Research Foundation (DFG) under grant number 490989047, DFG FOR 5455 ”TLS-Defo”.

REFERENCES

Cheng, J., editor (2009). The Principles of Astronomical Telescope Design. Astrophysics and Space Science Library. Springer New York, New York, NY. https://doi.org/10.1007/b105475

Clark, T. A. and Thomsen, P. (1988). Deformations in VLBI antennas. NASA Technical Memorandum 100696, Goddard Space Flight Center, Greenbelt, MD, USA.

Combrinck, L., Gaylard, M., Quick, J., and Nickola, M. (2011). Hartebeesthoek radio astronomy observatory (HartRAO). In Behrend, D. and Baver, K., editors, International VLBI Service for Geodesy and Astrometry 2010 Annual Report, NASA/TP-2011-215880.

Fraser, C. S. (1986). Microwave antenna measurement. Photogrammetric Engineering and Remote Sensing, 52(19):1627–1635.

Holst, C., Medic, T., Nothnagel, A., and Kuhlmann, H. (2019). Analyzing shape deformation and rigid body movement of structures using commonly misaligned terrestrial laser scanners: the radio telescope case. 4th Joint International Symposium on Deformation Monitoring (JISDM), 15-17 May 2019, Athens, Greece.

Holst, C., Zeimetz, P., Nothnagel, A., Schauerte, W., and Kuhlmann, H. (2012). Estimation of focal length variations of a 100-m radio telescope's main reflector by laser scanner measurements. Journal of Surveying Engineering, 138(3):126–135. https://doi.org/10.1061/(ASCE)SU.1943-5428.0000082

International VLBI Service for Geodesy and Astrometry (2026). International VLBI service for geodesy and astrometry: Components - network stations. https://ivscc.gsfc.nasa.gov/about/org/components/ns-list.html (27.01.2026)

Lösler, M., Eschelbach, C., Greiwe, A., Zhou, B., and McCallum, L. (2025). Innovative approach for modelling gravity-induced signal path variations of VLBI radio telescopes. Earth, Planets and Space, 77(1). https://doi.org/10.1186/s40623-024-02110-8

National Research Foundation (2026a). About SARAO Hartebeesthoek site. https://www.sarao.ac.za/about/hartrao/ (27.01.2026)

National Research Foundation (2026b). HartRAO 26m Radio Telescope Details. http://www.hartrao.ac.za/hh26m_factsfile.html (27.01.2026)

Nothnagel, A. (2009). Conventions on thermal expansion modelling of radio telescopes for geodetic and astrometric VLBI. Journal of Geodesy, 83(8):787–792. https://doi.org/10.1007/s00190-008-0284-z

Nothnagel, A. (2020). Very long baseline interferometry. In Freeden, W., editor, Mathematische Geodäsie/Mathematical Geodesy, Springer Reference Naturwissenschaften, pages 1257–1314. Springer Berlin Heidelberg, Berlin, Heidelberg. https://doi.org/10.1007/978-3-662-55854-6_110

Nothnagel, A., Holst, C., and Haas, R. (2019). A VLBI delay model for gravitational deformations of the Onsala 20 m radio telescope and the impact on its global coordinates. Journal of Geodesy, 93(10):2019–2036. https://doi.org/10.1007/s00190-019-01299-x

Pfaffinger, T., Rincón, M. A. O., Nothnagel, A., Mey, P., Quick, J., Botha, R., Stronkhorst, P., Nickola, M., and Holst, C.(2025) Quality-controlled deformation analysis of the 26-m HartRAO radio telescope's main reflector: First results. 6th Joint International Symposium on Deformation Monitoring (JISDM), 7-9 April 2025, Karlsruhe, Germany. https://doi.org/10.5445/IR/1000179768

Sarti, P., Abbondanza, C., Petrov, L., and Negusini, M. (2011). Height bias and scale effect induced by antenna gravitational deformations in geodetic VLBI data analysis. Journal of Geodesy, 85(1):1–8. https://doi.org/10.1007/s00190-010-0410-6

Sarti, P., Vittuari, L., and Abbondanza, C. (2009). Laser scanner and terrestrial surveying applied to gravitational deformation monitoring of large VLBI telescopes' primary reflector. Journal of Surveying Engineering, 135(4):136–148. https://doi.org/10.1061/(ASCE)SU.1943-5428.0000008

BIOGRAPHICAL NOTES

Theresa Pfaffinger, M. Sc.

Since 2024	Ph.D-Student and research assistant at Chair of Engineering Geodesy (Technical University of Munich)
2024	M. Sc. in Geodesy and Geoinformation (Technical University of Munich)
2021	B. Sc. in Geodesy and Geoinformation (Technical University of Munich)

Dr.-Ing. habil. **Axel Nothnagel**

Since 2019	VLBI Consultant at TU Wien, Department of Geodesy and Geoinformation, Austria
1999-2019	Associate Professor at University of Bonn, Germany
1999	Habilitation (University of Bonn)
1991	Dr.-Ing. (University of Bonn)
1982	Dipl.-Ing. (University of Bonn)

Prof. Dr.-Ing. **Christoph Holst**

Since 2021	Full Professor at Chair of Engineering Geodesy (Technical University of Munich)
2015	Dr.-Ing. (University of Bonn)
2010	M. Sc. in Geodesy and Geoinformation (University of Bonn)
2008	B. Sc. in Geodesy and Geoinformation (University of Bonn)

CONTACTS

Theresa Pfaffinger and Christoph Holst
Chair of Engineering Geodesy, TUM School of Engineering and Design, Technical University of Munich
Arcisstraße 21, 80333 Munich, GERMANY
Tel. +49 89 289 22851
Email: theresa.pfaffinger@tum.de, christoph.holst@tum.de
Web site: https://www.asg.ed.tum.de/gds/team/

Axel Nothnagel
Research Area Higher Geodesy, Department of Geodesy and Geoinformation, TU Wien, Austria
Wiedner Hauptstraße 8-10, 1040 Vienna, AUSTRIA
Tel. +43 1 58801 12860
Email: axel.nothnagel@tuwien.ac.at
Web site: https://www.tuwien.at/mg/geo/team